

2009

Estimation of the quasi-static Young's modulus of the rat eardrum using a pressurization method

Seyedeh Nastaran Ghadarghadar Jahromi

Follow this and additional works at: <https://ir.lib.uwo.ca/digitizedtheses>

Recommended Citation

Ghadarghadar Jahromi, Seyedeh Nastaran, "Estimation of the quasi-static Young's modulus of the rat eardrum using a pressurization method" (2009). *Digitized Theses*. 3966.
<https://ir.lib.uwo.ca/digitizedtheses/3966>

This Thesis is brought to you for free and open access by the Digitized Special Collections at Scholarship@Western. It has been accepted for inclusion in Digitized Theses by an authorized administrator of Scholarship@Western. For more information, please contact wlsadmin@uwo.ca.

**Estimation of the quasi-static Young's modulus of the rat eardrum
using a pressurization method**

(Spine title: Estimation of the quasi-static Young's modulus of rat eardrum)

(Thesis format: Integrated-Article)

by

Seyedeh Nastaran Ghadarghadar Jahromi

Graduate Program in Engineering Science, Department of Electrical and Computer
Engineering

A thesis submitted in partial fulfillment
of the requirements for the degree of
Master of Engineering Science

School of Graduate and Postdoctoral Studies
The University of Western Ontario
London, Ontario, Canada

© Seyedeh Nastaran Ghadarghadar Jahromi 2009

Abstract

Accurate estimates of the quasi-static Young's modulus of the eardrum are important for finite-element (FE) modeling of clinical procedures such as tympanometry or myringotomy. Tympanometry is a medical examination used to test the middle ear condition by creating variations of air pressure in the ear canal. Myringotomy is a surgical procedure in which a tiny incision is created in the eardrum, so as to relieve pressure caused by the excessive buildup of fluid. Although a few authors have reported estimates of the quasi-static Young's modulus, simplifying assumptions in the analytical approaches may raise questions as to the accuracy of the various methodologies. The objective of this project is to develop a method for estimating the quasi-static Young's modulus of the rat eardrum from pressurized shape measurements made using Fourier transform profilometry and optimization of a FE model. First the technique was validated on a synthetic membrane with properties similar to the eardrum. As a synthetic membrane we used five soft contact lenses. A pressurization system was used to apply quasi-static pressures up to 4 kPa to each contact lens. The resting and deformed shapes of each lens were measured using a Fourier transform profilometer, a non-contacting optical device for shape measurements. A FE model was constructed for each contact lens from the resting shape data, and the Golden-Section optimization technique was used to automatically find the Young's modulus of the contact lens model. The average value estimated for the contact lenses was 1.33 ± 0.02 MPa which is within the range of values reported for this type of contact lens (1.2 to 1.4 MPa). Finally after technique validation, measurements were made on six rat eardrums with immobilized ossicular chains. The same procedure as for the contact lens was

used to measure the eardrum Young's modulus. For the six eardrum samples, an average value of 22.8 ± 1.5 MPa was obtained for the Young's modulus, which is comparable to values found in the literature. Moreover, the results are repeatable as indicated by the low standard deviation.

Keywords: Contact lens, Eardrum, Young's modulus, Pressurization technique, Finite element model, Optimization technique

Co-authorship

Chapter 2 of the thesis contains a manuscript prepared for submission to *The Journal of the Association for Research in Otolaryngology* entitled "Estimation of the quasi-static Young's modulus of the rat eardrum using a pressurization technique". It was co-authored by Seyedeh Nastaran Ghadarghadar Jahromi, Dr. Sumit Agrawal, Dr. Abbas Samani and Dr. Hanif Ladak. Nastaran Ghadarghadar, the Master's candidate, implemented the required hardware and software and conducted the experiments and validity studies. Dr. Ladak and Dr. Samani were the supervisors for Nastaran Ghadarghadar, and provided the objectives and directions for the project. Dr. Agrawal, an ear surgeon, provided training for rat ear surgery and helped with dissections and sample preparation.

Acknowledgments

I appreciate the guidance of my supervisors Dr. Abbas Samani and Dr. Hanif Ladak in this project. I would also like to thank late Dr. Suzanne Bernier for providing the rats used in this research project and Dr. Sumit Agrawal for his training and assistance in rat dissection and sample preparation. I would also like to thank all my colleagues in my lab especially Hatf Mehrabian, Iman khalaji and Mohammad Hesabgar who helped me in FE modeling and sample preparation.

I would also like to thank the funding sources of this project, the Natural Sciences and Engineering Research Council of Canada (NSERC) and Western Engineering Scholarship (WES) provided by the University of Western Ontario.

To my mother, for her unsparing support and encouragement.

Contents

CERTIFICATE OF EXAMINATION	iii
Abstract	iii
Co-Authorship	vi
Acknowledgments.....	vi
Dedication.....	vii
Contents	viii
Table of Figures.....	x
1 Chapter 1 (Introduction)	1
1.1 Hearing disorders.....	1
1.1.1 Consequences of Hearing Disorder in Life	1
1.1.2 Hearing disorder statistics.....	2
1.2 Research motivation	4
1.3 Human ear anatomy	6
1.3.1 The external ear.....	7
1.3.2 The eardrum or tympanic membrane	7
1.3.3 The eardrum structure	9
1.3.4 The middle ear or tympanic cavity and the auditory ossicles.....	9
1.3.5 The internal ear or labyrinth	10
1.4 Mechanism of hearing	12
1.5 Rat eardrum.....	13
1.6 Eardrum's stiffness parameters.....	14
1.7 Measurement of soft tissues' Young's modulus	15
1.8 Thesis outline.....	18
1.9 References	19
2 Chapter 2 (Paper manuscript)	22
2.1 Introduction.....	22
2.2 Technique validation.....	26
2.2.1 Synthetic membrane.....	26
2.2.2 Pressurization apparatus.....	26
2.2.3 Experimental procedure	28

2.2.4	FE model	29
2.2.5	Optimization	31
2.3	Application to eardrum	32
2.4	Results	36
2.4.1	Validation	36
2.4.2	Application to eardrum	40
2.5	Discussion	44
2.5.1	Validation	44
2.5.2	Application to eardrum	45
2.6	Conclusion	49
2.7	References	50
3	Chapter 3 (Summary, conclusion and future work)	55
3.1	Summary.....	55
3.1.1	Contact lens phantom study	56
3.1.2	Rat eardrum study	56
3.2	discussion and future work	57
3.2.1	Thickness distribution	57
3.2.2	Inhomogeneity.....	58
3.2.3	Anisotropy	58
3.2.4	Tissue intrinsic nonlinearity.....	59
3.2.5	Further eardrum's FE model refinement	59
3.3	References	60
	Curriculum Vitae	62

Table of Figures

Figure 1.1. Schematic of external and middle ear.....	6
Figure 1.2. Schematic of right tympanic membrane	7
Figure 1.3. Schematic of the auditory ossicles	10
Figure 1.4. Schematic of right interior ear	11
Figure 1.5. Mechanism of hearing	13
Figure 1.6. Comparison between rat and human eardrum	14
Figure 2.1. Schematic of pressurization apparatus used for contact lens.....	27
Figure 2.2. Radial profiles through contact lens at different pressures	30
Figure 2.3. Sample FE model of the rat eardrum	35
Figure 2.4. Sample FE model of a contact lens.....	38
Figure 2.5. Radial profiles of contact lens	38
Figure 2.6. Full-field error map of contact lens	39
Figure 2.7. Objective function vs. Young's modulus for contact lens	39
Figure 2.8. Effect of thickness on Young's modulus	40
Figure 2.9. Shape profiles of eardrum at different sections	42
Figure 2.10. Full-field error map of eardrum	43
Figure 2.11. Objective function vs. Young's modulus for eardrum.....	43

Chapter 1

Introduction

In this chapter some facts and statistics regarding hearing disorders and their effects on the quality of life are presented. This will set the stage for the motivation of the presented research. This chapter also includes a description of ear anatomy followed by an overview of the mechanical properties of the eardrum.

1.1. Hearing Disorders

Hearing disorder is defined as complete or partial inability to hear and recognize sounds. Hearing disorder has different levels: soft, moderate and severe. Deafness is regarded as severe hearing disorder. A deaf person cannot hear completely from one of the ears or both.

1.1.1. Consequences of Hearing Disorder in Life

Hearing has a critical role in many aspects of life. Talking, learning and communication skills are some of these aspects that hearing has a direct impact on. Therefore, hearing disorders and deafness could cause serious issues in an individual's life and at a larger scale in societies and countries.

Children with hearing problems have a hard time communicating with others and develop their academic abilities. Also, it would be more difficult for adults to find a job and keep their employment while having hearing problems, leading individuals with such problems to be socially withdrawn and consequently having low self esteem. Usually hearing disorders are more prevalent among the less privileged, because they are not able to afford paying for essential ear health care expenses (World Health Organization (WHO), 2005). Additionally, if the less privileged have hearing problems, they will not be able to afford hearing instruments necessary for improving their hearing. Since hearing problems lead to inevitable negative impact on learning and education and consequently inability to obtain high paying jobs, it would be harder for this class of people to escape poverty. Moreover, it is relatively expensive to provide special education to people with hearing problems as it involves expensive educational equipment. Considering all these facts, hearing disorders can impose a heavy economic burden on societies.

1.1.2. Hearing Disorder Statistics

More than 278 million people all over the world have moderate to severe hearing impairment in both ears. Eighty percent of the deaf people and people with hearing problems live in countries where the average income is low or moderate. Although fifty percent of hearing problems could be prevented by avoidance and early

diagnosis, the number of people having hearing problems is growing because of the rising number of people living worldwide in addition to inability of the poor to prevent hearing loss. Statistics show that in developing countries, less than 0.025% of the people who need hearing instruments can afford obtaining them. Furthermore, the number of hearing instruments produced annually is less than 10% of worldwide requirements (World Health Organization (WHO), 2005). All in all, these statistics and numbers indicate the importance of developing effective and affordable methods of treating hearing disorders. This is only possible by better understanding of our auditory system.

The main source of soft and moderate hearing disorders in children is injury or infection of the middle ear. The effect of middle ear infection on different phases of a child's life is dependent on the severity of the hearing disorder as well as the age in which hearing disorder occurs.

As statistics show there are quite a large number of people who suffer from hearing disorders. Mainly, there are three types of hearing disorders based on where the damage in the auditory system is: conductive hearing impairment, sensorineural hearing impairment and mixed hearing impairment (Moller, 2006). Conductive hearing impairment is due to a problem in the outer ear, middle ear, tympanic membrane or the middle-ear ossicles. It usually causes a reduction in hearing level and could be treated medically or surgically. Sensorineural hearing loss refers to a hearing problem in the

inner ear (cochlea) and the hearing nerves going from the inner ear to the brain. This type of hearing disorder is permanent and cannot be treated medically or surgically. It can be caused by different factors such as aging or noise exposure. The third type of hearing disorder is mixed hearing loss which is a combination of both conductive and sensorineural hearing loss, which happens when there is a hearing problem in the outer or middle ear as well as in the inner ear or hearing nerves.

1.2. Research Motivation

One of the common ways to model the ear is using finite element models. The Finite Element Method (FEM) is a numerical method to find approximate solutions of partial differential equations (PDEs). FEM discretizes the domain by meshing the object into smaller portions called finite elements. Using some approximations, the governing PDEs are converted into a small system of algebraic equations valid within the domain of each element. These equations are assembled to form a larger system of equations that govern the whole domain. After applying the boundary conditions, this system of equations is solved to determine the unknown field, e.g. displacement, temperature, velocity, etc. FEM is used in biomechanical modeling of biological tissues. This includes conducting auditory experiments via simulation, understanding the underlying mechanisms of hearing and predicting hearing level after performing ear surgical procedures.

One of the main factors in modeling the middle ear using FEM is to have accurate estimation of the eardrum's Young's modulus, which is a numerical representation of its stiffness.

Previously, scientists have attempted measuring the Young's modulus (YM) of the eardrum by using different techniques. Some estimated the quasi-static YM while the others claimed to have measured the dynamic YM of the eardrum. However, experimental protocols and simplifying assumptions used in their experimental data analysis techniques may have had a negative impact on the accuracy of their estimated YM values. In this research, we proposed a new, accurate and repeatable technique for measuring the YM of the eardrum. One of the applications of having an accurate estimate of the quasi-static YM is in tympanometry in which the acoustic admittance of the middle ear is measured at the eardrum as a function of quasi-static pressure applied to the eardrum. The accuracy of models of the eardrum and middle ear depends critically on the accuracy of the eardrum's YM. Accurate quasi-static models would be useful for interpreting tympanometric data (Daniel *et al*, 2001). Another application is simulating surgical procedures such as myringotomy, a surgical operation in which a tiny opening is made in the eardrum. Accurate models could be used to improve the procedure and could be used in virtual reality environments for training surgical residents.

To have a better understanding of the structure and functionality of the ear, the ear anatomy and hearing mechanism are reviewed in the next section.

1.3. Human Ear Anatomy

The human ear anatomy is shown in Figure 1.1. From an anatomical point of view, the human ear has three major parts: The external ear, middle ear and internal ear (Gray, 1918). As our area of interest in this study is middle ear and especially the eardrum, the anatomy of the middle ear as well as the eardrum is discussed in more detail.

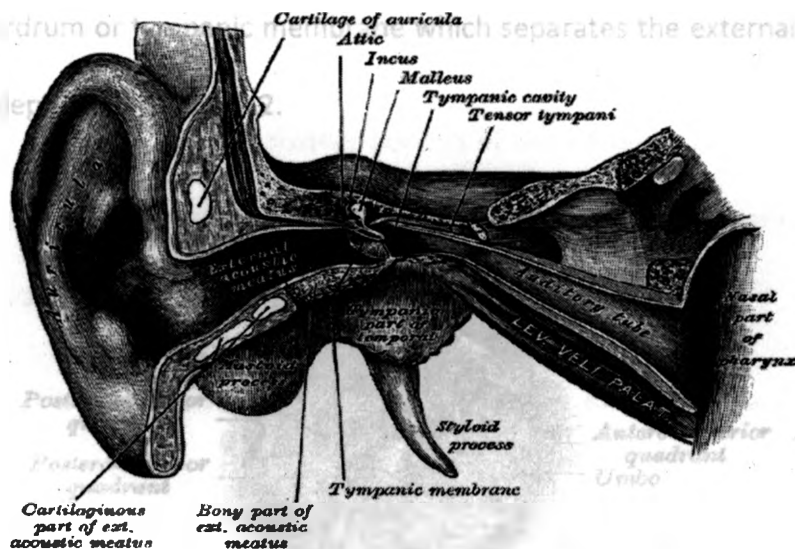


Figure 1.1: Schematic of external and middle ear. This image is a reproduction of a lithograph plate from a 1918 version of Gray's Anatomy, and is in the public domain.

1.3.1. The External Ear

The external ear is made up of two major parts: the pinna or the auricle and the ear canal or external acoustic meatus (Gray, 1918). The pinna or auricle is the visible part of the ear which collects and amplifies sound energy. One end of the ear canal is attached to the auricle and the other end is attached to the middle ear via the eardrum. Sound energy is transmitted from the auricle to the middle ear via the tympanic membrane.

1.3.2. The Eardrum or Tympanic Membrane

The eardrum or tympanic membrane which separates the external ear from the middle ear is depicted in Figure 1.2.

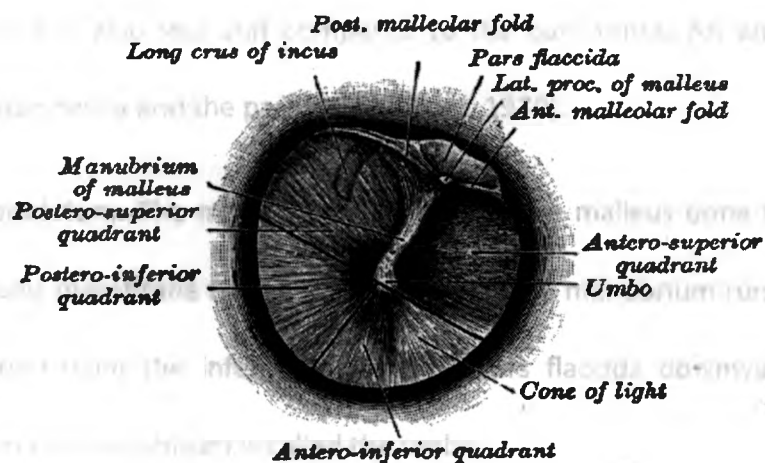


Figure 1.2: Schematic of right tympanic membrane. This image is a reproduction of a lithograph plate from a 1918 version of Gray's Anatomy, and is in the public domain.

The tympanic membrane is a membrane located at the end of the ear canal which separates the outer ear from the middle ear. The tympanic membrane is relatively thin (10's of microns thick), semitransparent and has an oval shape with major diameter of about 9 to 10 mm and minor diameter of 8 to 9 mm. It has a conical shape with its peak approximately in the middle (Decraemer *et al*, 1991). The tympanic membrane consists of three major parts:

Pars tensa: In humans most of the tympanic membrane consists of the pars tensa which is thicker than the rest of the tympanic membrane and mostly the eardrum is characterized based on the properties of this portion.

Pars flaccida: It is the top smaller portion of the eardrum which is thinner than the pars tensa. It is also less stiff compared to the pars tensa. An annular ligament separates the pars tensa and the pars flaccida (Lim, 1970).

The manubrium: The manubrium is a part of the malleus bone that is coupled with the tympanic membrane from the medial side. The manubrium runs in the infero-superior direction from the inferior end of the pars flaccida downwards. The most inferior point on the manubrium is called the umbo.

1.3.3. The Eardrum Structure

The eardrum is a membrane that consists of three layers: Epidermis on the outside, lamina propria and mucosal layer on the inside. The lamina propria itself is made of four layers: Subepidermal connective tissue, outer layer of radial fibres, inner layer of circular fibres and submucosal connective tissue (Lim, 1995).

1.3.4. The Middle Ear or Tympanic Cavity and the Auditory Ossicles

The middle ear is the part of the ear between the eardrum and the inner ear (cochlea). Other names of the middle ear are tympanic cavity or cavum tympani (Gray, 1918). The middle ear volume is approximately 2 cubic centimetres and is filled by air. It consists of the three auditory ossicles (malleus, incus and stapes). The opening of the eustachian tube is in the middle ear. The eustachian tube is approximately 35 mm long extending from the back of the nasal cavity to the middle ear. It ventilates the middle ear cavity to keep its pressure near ambient pressure (Gray, 1918).

The three movable auditory ossicles are named after their shapes. These ossicles are illustrated in Figure 1.3. The most lateral ossicle is the malleus (or hammer). As shown in this figure, the manubrium of the malleus is attached to the eardrum as was described before and the other end is attached to the incus (or anvil). The incus itself is attached to the stapes (or stirrup) which is the smallest bone in the human body.

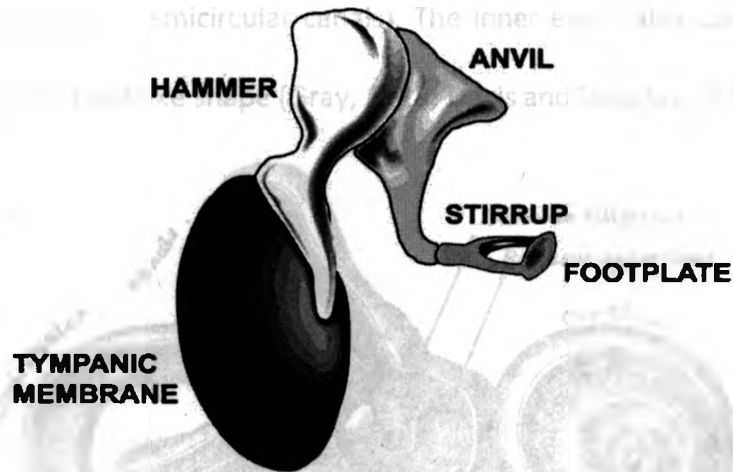


Figure 1.3: Schematic of auditory ossicles attached to the tympanic membrane. This image is a reproduction of www.psywww.com/.../ch04_senses/04ossicles.jpg.

When sound energy goes through the ear canal it causes the eardrum to vibrate. The vibration of eardrum causes the vibration of malleus as it is attached to the eardrum via the manubrium. This vibration is transferred to the incus and then to the stapes. Finally, the vibration of the stapes causes the movement of the fluid in the cochlea where the vibrations of the fluid are converted into electrical signals, which are transmitted to the brain.

1.3.5. The Internal Ear or Labyrinth

The internal ear is illustrated in Figure 1.4. It is located at the end of the middle ear and consists of two major components: the cochlea and the vestibule apparatus

(vestibule and the three semicircular canals). The inner ear is also called the labyrinth because of its coiled snail-like shape (Gray, 1918; Davis and Douglass, 1905).

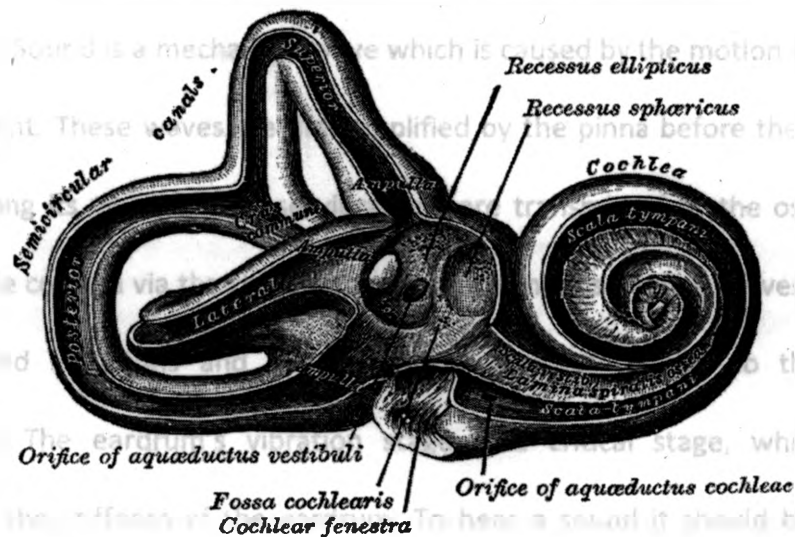


Figure 1.4: Schematic of right internal ear. This image is a reproduction of a lithograph plate from a 1918 version of Gray's Anatomy, and is in the public domain.

The cochlea is filled with fluid and is called the hearing organ. When the three ossicles vibrate, the vibration causes the fluid in the cochlea to vibrate. Hence, this vibration is transmitted to the hair cells that cover the interior part of the cochlea. The vibration of the hair cells generates nerve impulses which are transmitted to the brain along the auditory nerve and the brain interprets them as sounds that we can hear.

The main functionality of the vestibule and the three semicircular canals is to help the body maintain its balance in different situations.

1.4. Mechanism of Hearing

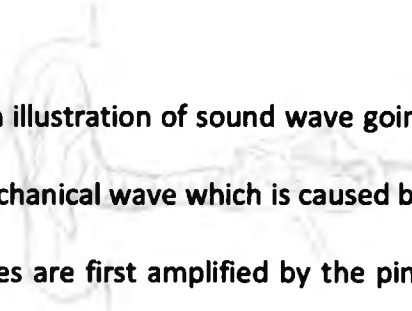


Figure 1.5 presents an illustration of sound wave going through the external ear and ear canal. Sound is a mechanical wave which is caused by the motion of particles in the environment. These waves are first amplified by the pinna before they impact the eardrum causing its vibration. These vibrations are transmitted to the ossicular chain and then to the cochlea via the stapes. The cochlea contains hearing nerves that pick up the transmitted vibrations and send them as electrical signals to the brain for interpretation. The eardrum's vibration stage is a critical stage, which is highly influenced by the stiffness of the eardrum. To hear a sound it should be within the frequencies which are recognizable for the ear. These frequencies are determined by the stiffness of the eardrum that can be characterized by the YM. This highlights the importance of the eardrum's YM and the motivation for its measurement. The range of frequencies that humans can hear is between 12 Hz to 20 KHz. However, aging is normally associated with change in tissue stiffness leading to decrease in the upper bound of this frequency range. Other animals have different ranges of hearing frequencies.

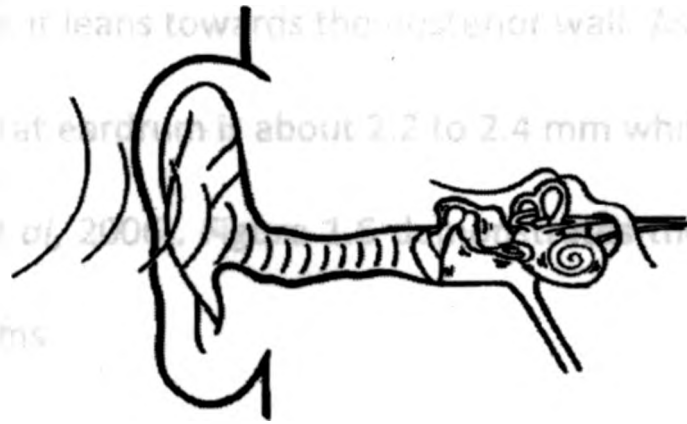


Figure 1.5: mechanism of hearing. The pinna amplifies sound energy and conducts it to the ear canal. Finally the sound wave is transmitted to the cochlea via the eardrum and the ossicles. This image is a reproduction of http://www.hearing.com.au/digitalAssets/2192_1109219334458_howearswork.gif.

1.5. Rat Eardrum

In the present study we used rat temporal bone specimens. This was motivated by the fact that many researchers in the hearing scientific community use the rat as their animal model. The structure and mechanism of rat ear is very similar to the human ear but at a smaller scale (Hellstrom *et al*, 1982). Since this investigation studies the acoustic properties of the eardrum, a general description of tissue mechanical parameters and mechanical properties of the rat eardrum, a comparison between the rat and human eardrum is necessary.

While in humans, the area of pars flaccida is only 3-6% of the area of pars tensa, in rats, the area ratio is much larger and it is about 25-29%. In rat the short handle of the malleus points towards the posterior wall of eardrum while in humans it points toward the anterior wall. Moreover, the malleus in the rat is slightly curved towards the lower

wall whereas in human it leans towards the posterior wall. As a final point, the anterior-posterior diameter of rat eardrum is about 2.2 to 2.4 mm while in human it is about 9 to 10.2 mm (Castagno *et al*, 2006). Figure 1.6 demonstrates the differences between the rat and human eardrums.

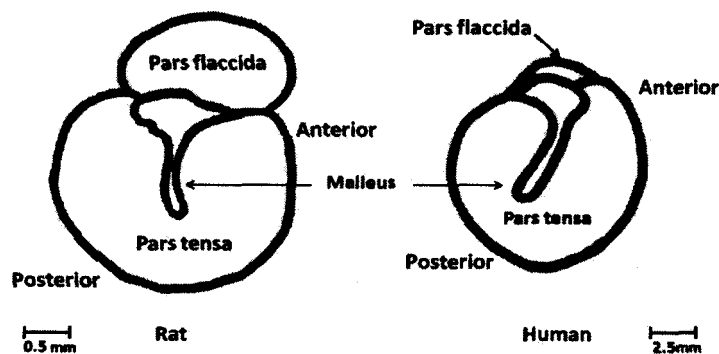


Figure 1.6: Comparison between rat and human eardrum.

As the objective of the present study is to estimate the quasi-static Young's modulus of the eardrum, a general description of tissue mechanical parameters and their measurement techniques is given in the following sections.

1.6. Eardrum's Stiffness Parameters

The eardrum's stiffness can be characterized by a number of parameters depending on how its mechanical response is idealized. This idealization ranges from isotropic and linear elastic (Bèkèsy, 1960; Gaihede *et al*, 2007) to orthotropic and linear elastic (Fay *et al*, 2005). In the isotropic linear elastic model, the stiffness is

characterized by two parameters, which are the YM and Poisson's ratio. The YM can be defined as the growth of stress required to induce a unit strain. Using various techniques described in the following section, researchers have obtained values that span a wide range of 7.0 MPa to 400 MPa obtained by Gaihede *et al* (2007) and Fay *et al* (2005), respectively. The Poisson's ratio is defined to characterize the material's volume change as a result of deformation. If a loading is applied in a certain direction, the tendency of the material to somewhat preserve its original volume dictates that the material is deformed in the perpendicular direction in addition to its deformation in the direction of loading. As such, the Poisson's ratio is defined as the negative ratio of the strain in the perpendicular direction to the strain in the direction of loading. The range of Poisson's ratio is from about 0.3 for isotropic crystalline solids to 0.5 for rubberlike materials (Snowdon, 1968). The latter is considered incompressible. Given that the bending is predominant in the eardrum's physiological deformation, its mechanical behaviour is probably not very sensitive to the value of the Poisson's ratio (Funnell, 1975). Since no experimental data is available for the eardrum's Poisson's ratio and given the small sensitivity of the eardrum's behaviour to its value, a value of 0.3 was considered in this research.

1.7. Measurement of Soft Tissues' Young's modulus

The YM of soft tissues can be measured using conventional methods such as uniaxial and beam bending tests. In the following, the basic principles of these methods

and their limitations are discussed. These limitations set the motivation to develop a new technique for measuring the YM of rat eardrum.

In the uniaxial test a tissue specimen is cut into a cylindrical shape. The two ends of the specimen are gripped by the testing machine, which is programmed to apply tensile or compression force to the specimen via the grips. The machine allows measuring and recording the applied forces and the resulting changes in the specimen's length. Using the recorded forces and the cross sectional area of the specimen, the stresses are calculated, and using the length changes and the original length the corresponding strains are calculated. Hence, the stress is plotted against the strain and the slope of the initial linear portion of the resulting curve is regarded as the tissue's YM. For eardrum specimens, the tissue is cut into strips, which are fixed from one end while stretched gradually from the other end. Similarly, the stresses are plotted against the strains and the slope of the initial linear portion is calculated to obtain the eardrum's YM.

The beam bending test is usually used with bone YM measurement. It involves applying bending using point forces to the bone which is assumed to have uniform cross section throughout its length. The forces are gradually applied while the deflections underneath the forces are measured. Hence, the forces are plotted against the deflections and the YM is calculated from the slope of the plotted forces vs. deflection relationship as it is proportional to this slope. For eardrum, a strip of soft tissue is cut

and one of its ends is fixed while the other end is free to form a beam that can be idealized as a cantilever beam. At the free end, incrementally increasing forces perpendicular to the beam's longitudinal axis are applied while the resulting deflections at this end are measured. Similarly, the YM of the eardrum can be calculated from the plot of the force vs. deflection curve. Both of the uniaxial and bending test methods have major problems which compromise their accuracy in measuring the eardrum's YM. The main issue in these methods is that they both involve cutting the tissue to obtain regular cylindrical or strip shape specimens leading to compromising the eardrum's structural integrity, thus altering its mechanical properties. The other major issue is related to the specimens' boundary condition effects which render the stress and strain distributions non-uniform within the specimens. The boundary condition effects are particularly more important in the context of eardrum YM measurement because only short samples, the length of which is dictated by the eardrum's diameter, can be cut and tested. This implies that a significant portion of the specimen would be influenced by the fixed boundaries leading to stress and strain non-uniformity within the tissue. To address the issues of the conventional uniaxial and bending tests, other groups including our group (Samani *et al*, 2003) have developed indentation techniques to measure tissues' YM. This technique does not require tissue cutting as it involves indenting the tissue while it is intact. The response of the respective experiment is characterized by applied indentation displacements and their corresponding forces, which are acquired

and processed to determine the tissue's YM. The loading involved in the indentation experiment leads to non-uniform stress and strain distributions. This non-uniformity is taken into account in the model used to process the acquired data as described by Samani *et al* (2003). Another alternative that also avoids tissue cutting and its consequences is pressurization method, which has been used in this research. This technique involves pressurizing the eardrum at various pressure levels and measuring the corresponding eardrum's shape. This pressure-shape information is processed using an optimization algorithm as described in details in Chapter 2 to determine the YM.

1.8. Thesis Outline

Because of the significance of eardrum's YM in its FE modeling, we proposed a new technique for measuring the eardrum's YM which does not involve cutting the tissue. It engages a very accurate FE model which takes into account the three dimensional geometry of the eardrum as well as geometric nonlinearity. Furthermore the FE model does not involve the complexity of the contact problem which is the case in the indentation technique reported by our group (Samani *et al*, 2003).

Chapter 2 of the thesis contains a paper manuscript. In this paper, initially the precision and achievability of the pressurization technique was examined performing a phantom study. For the phantom study, five soft contact lenses were used. Subsequently the technique was applied to the rat eardrum to measure its stiffness.

Measurements were made on six rat eardrums with immobilized ossicular chains. A pressurization system was used to apply quasi-static pressures up to 4 kPa to each eardrum. The resting and deformed shapes of each eardrum were measured using a Fourier transform profilometer, a non-contacting optical device for shape measurements. A FE model was constructed for each eardrum from the resting shape data, and the Golden-Section optimization technique was used to automatically find the Young's modulus of the model eardrum. The estimation technique proposed in this work yields Young's modulus values that are comparable to those reported in the literature for other species. Details about sample preparation, pressurization apparatus, pressurization measurement, and finite element model construction are discussed in chapter 2 of the thesis.

Chapter 3 summarizes the work presented in chapter 2. By making a conclusion on the assumptions made, chapter 3 gives a direction for further studies in this area.

1.9. References

Békésy, G.v., 1960. Experiments in Hearing, McGraw-Hill, Toronto, ON.

Castagno.L.A., Lavinsky.L., 2006. Tympanic membrane healing in myringotomies performed with argon laser or microknife: an experimental study in rats, Rev Bras Otorrinolaringol., 72(6) 794-799.

- Daniel, S.J., Funnell, W.R.J., Zeitouni, A.G., Schloss, M.D., Rappaport, J., 2001. Clinical applications of a finite-element model of the human middle ear., *The Journal of Otolaryngology*, 30 (6) 340-346.
- Davis, A.D., Douglass. B., 1905. *Eye, Ear, Nose, and Throat Nursing*, Harvard University, USA.
- Decraemer, W.F., Dircks, J.J.J., Funnell, W.R.J., 1991. Shape and derived geometrical parameters of the adult, human tympanic membrane measured with a phase-shift moiré interferometer., *Hear.Res.* (51) 107-121
- Fay, J., Puria, S., Decraemer, W.F., Steele, C., 2005. Three approaches for estimating the elastic modulus of the tympanic membrane. *J. Biomech.*, 38 (9) 1807-1815.
- Funnell, W.R.J., Laszlo, C.A., 1975. Modelling the eardrum as a doubly curved shell using the finite-element method. *J. Acoust. Soc. Am.* 57 Suppl (72)
- Gaihede, M., Liao, D., Gregersen, H., 2007. In vivo areal modulus of elasticity estimation of the human tympanic membrane system: modelling of middle ear mechanical function in normal young and aged ears. *Phys. Med. Biol.*, 52 (3) 803-814.
- Gray, H., 1918. *Anatomy of the human body*, Philadelphia, USA.
- Hellstrom S., Salen B., Stenfors L., 1982. Anatomy of the rat middle ear. *Acta Anat (Basel)*, (112) 346-52.
- Lim, D.J., 1970. Tympanic membrane. An ultrastructural observation., *Acta Otolaryng.*, (70), 176-186
- Lim, D.J., 1995. Structure and function of the tympanic membrane: a review. *Acta Oto-Rhino-Laryngologica Belgica.*, (49) 2 101-15

Moller, A.R., 2006. Hearing: Anatomy, Physiology, and Disorders of the Auditory System., Dallas, Texas, US.

Samani, A., Bishop, J., Luginbuhl, C., Plewes, D.B., 2003. Measuring the elastic modulus of ex vivo small tissue samples. *Phys. Med. Biol.*, 48 (14) 2183-2198

Snowdon, J.C., 1968. Vibration and shock in damped mechanical systems., Wiley, New York, USA.

World Health Organization (WHO)., 2005. Fact sheets of deafness and hearing impairment.

Chapter 2

Estimation of the quasi-static Young's modulus of the rat eardrum using a pressurization technique

(Prepared for Submission to: *The Journal of the Association for Research in Otolaryngology*)

2.1. Introduction

Myringotomy is a surgical procedure in which a small incision is made in the eardrum to alleviate ear infections. Myringotomy with tube insertion is used to treat middle-ear infections, and is the most common surgical procedure in the United States next to circumcision for children under 15 years of age (Pokras *et al*, 1997). Surgical residents are taught the procedure at a very early stage through observations and limited practice on patients. However, a high level of dexterity, practice, and experience are needed to operate under a microscope, insert a blade through the narrow ear canal, and create the incision.

Over the last few decades, virtual-reality (VR) technology consisting of computers and 3D human-computer interfaces has been utilized to simulate various surgical procedures for training purposes. The major benefits of VR-based surgical simulation include patient safety, broadening surgical training through the provision of

different virtual patient types, and its ability to quantify surgical performance (Fried *et al*, 2007). Recently, we reported the first VR-based simulator for training in myringotomy (Leigh *et al*, 2009). In the current implementation, the eardrum is treated as a static structure: It does not deform and then perforate when contact is made with a virtual myringotomy blade. However, a user evaluation questionnaire administered to surgical staff and senior surgical residents indicated that simulating the deformation would greatly add to the realism of the simulator and would provide clues to the trainee with regard to the amount of force required to perforate the eardrum.

The finite-element (FE) method has been used to model both the quasi-static (Ladak *et al*, 2006) and dynamic (e.g., Tuck-Lee *et al*, 2008; Gan *et al.*, 2006; Koike *et al*, 2002; Beer *et al*, 1999; Eiber, 1999; Ferris and Prendergast, 1999; Funnell *et al*, 1987) mechanical behaviours of the eardrum. For surgical simulation, a quasi-static model is the most appropriate choice because movements during surgery are slow. For modeling quasi-static and low-frequency dynamics, isotropic models of the eardrum fit experimental data well (Elkhouri *et al*, 2006). Furthermore, even for fairly large loads, a linear elastic material model characterized by a single Young's modulus and Poisson's ratio is sufficient (Ladak *et al*, 2006).

The accuracy of linear elastic isotropic FE models depends critically on several modeling parameters, particularly the Young's modulus of the pars tensa portion of the

eardrum (Funnell and Laszlo, 1978). However, there is substantial disagreement in reported estimates of the Young's modulus of the eardrum. Several authors have reported estimates made using dynamic stimuli. Kirikae (1960) reported a value of 40 MPa for the Young's modulus of the human eardrum measured through uniaxial tensile testing by oscillating a strip of tissue at 890 Hz. Decraemer *et al* (1980) also performed uniaxial tension tests but used a stimulus frequency of 300 Hz and arrived at an estimate of 23 MPa. More recently, Fay *et al* (2005) made estimates taking into account the fibrous composite ultrastructure of the eardrum as well as non-uniformities in eardrum thickness. Their dynamic measurements suggest that the Young's modulus of the human eardrum lies in the range 0.1 to 0.3 GPa depending on the eardrum's region and layer (radial or circumferential), whereas that of the cat lies in the range of 0.1 to 0.4 GPa.

The Young's modulus of tissues varies with frequency (Fung, 1993), so one might anticipate the estimated Young's modulus of the eardrum to be different when considering static and quasi-static stimuli. Békésy (1960) reported a value of 20 MPa for the static Young's modulus of the human eardrum, whereas Gaihede *et al* (2007) reported an average value of 10.33 MPa amongst their older group of subjects and 6.88 MPa amongst their younger group. In an attempt to refine measurements of the eardrum's Young's modulus, we developed a technique in which force-displacement curves were measured using an indentation apparatus (Marshall *et al*, 2007), and the

Young's modulus of an FE model with subject-specific geometry was numerically optimized such that simulated force-displacement curves matched measured ones, thus yielding an estimate of the Young's modulus of the actual eardrum. Recently, Aernouts *et al* (2009) have presented an indentation technique similar to ours and applied it to the rabbit eardrum.

Simulating the indentation experiment of Hesabgar *et al* (2009) using an FE model involves contact modeling which is computationally expensive. In this work, we modified our previous indentation technique by using static pressures and measuring the pressurized shape of the eardrum. The use of air pressure avoids the need to apply direct forces to the eardrum, thereby avoiding the need for contact modeling. Subject-specific FE models were then used to estimate the Young's modulus by optimization of the models so that the deformed shape calculated by the models matched experimentally measured shapes. Here, the new technique is presented and validated by applying it to a synthetic membrane with a known Young's modulus. After validation, the technique was applied to actual rat eardrums.

2.2. Technique Validation

2.2.1. Synthetic membrane

The synthetic membrane used to test our methodology is a standard contact lens. Five CIBA Night and Day soft contact lenses (CIBA Vision Corporation, Duluth, GA, USA) were used. Each lens had a diameter of 13.8 mm and a base curve of 8.4 mm. Like an eardrum, a contact lens is a thin shell-like structure with a thickness that varies across its surface. Indeed, the eardrum is commonly modeled as a thin shell (Funnell and Laszlo, 1978). Although the typical mammalian eardrum has been described as an offset cone with sides of varying curvature (Funnell and Laszlo, 1982) whereas a contact lens is hemispherical, both have suitably complex shell-like geometries, which makes the contact lens a suitable choice for evaluating the accuracy of the proposed estimation method when applied to membranes with complex geometries. Furthermore, since our objective is to estimate an “effective” static Young’s modulus under the assumption of isotropy, a contact lens is a reasonable choice since its material properties are isotropic.

2.2.2. Pressurization Apparatus

Figure 2.1 shows a schematic diagram of the apparatus used to pressurize the contact lens. A specially constructed rigid chamber with a cap was used to house the contact lens as shown in Figure 2.1. The chamber was constructed so when the contact

lens was placed in it, the cap obscured the perimeter of the contact lens. This mimics the situation with a real eardrum in which the bony portion of the ear canal obscures the perimeter of the eardrum, making shape measurement of this part of the eardrum by optical methods as used in this work (see Section 2.2.3) impossible. Constructing the chamber and cap in this manner allowed us to determine if errors associated with extrapolation of shape measurements to the perimeter when constructing FE models had a significant effect on the estimated Young's modulus.

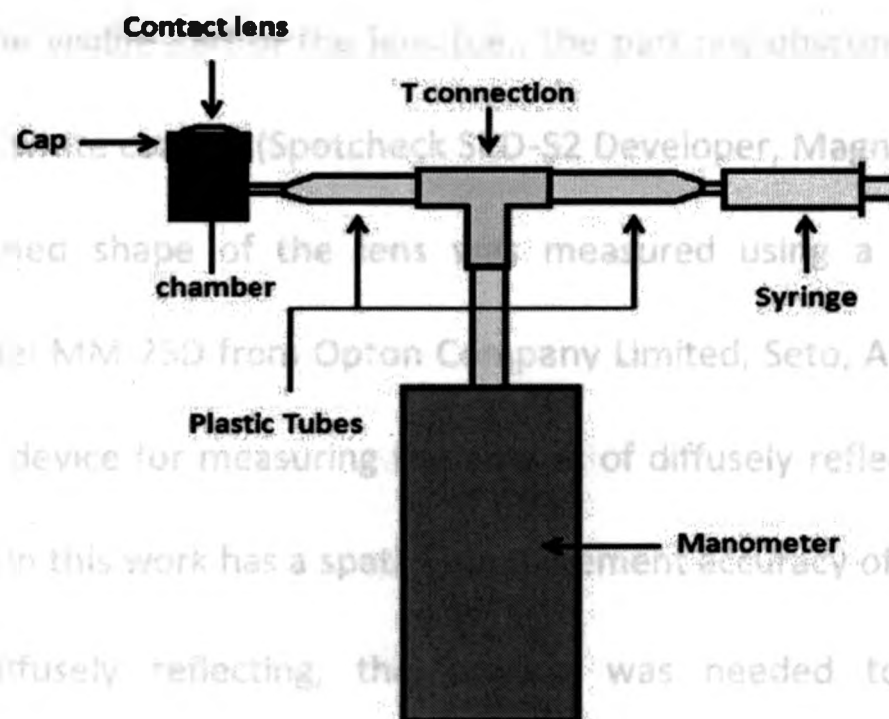


Figure 2.1: Schematic of the pressurization apparatus used for the contact lens.

A 3.0 mL syringe was used to manually apply pressure to the chamber and hence the lens. The pressure was monitored using a digital manometer (model HHP680 from

Omega, Quebec, Canada). The manometer has a resolution of 2.5 Pa for pressures less than approximately 2.49 kPa and 25.0 Pa for higher pressures.

2.2.3. Experimental Procedure

The perimeter of the lens was affixed to the chamber with glue to ensure the boundary of the lens did not move, and the cap was placed to create an air-tight seal. Before applying pressure to each lens, a thin coat of Vaseline (Unilever PLC, London, England) was applied to both sides of the lens to prevent dehydration during the measurements. The visible part of the lens (i.e., the part not obscured by the cap) was coated with a thin white coating (Spotcheck SKD-S2 Developer, Magnaflux, Glenview, IL) and the undeformed shape of the lens was measured using a Fourier transform profilometer (model MM-25D from Opton Company Limited, Seto, Aichi, Japan), a non-contacting optical device for measuring the shapes of diffusely reflecting surfaces. The profilometer used in this work has a spatial measurement accuracy of 10 μ m. Since the lens was not diffusely reflecting, the coating was needed to facilitate shape measurement. The effect of similar coatings on shape and deformation measurements has been shown to be negligible (Dirckx and Decraemer, 1997). The output of the profilometer is a dense cloud of triangulated points that represents the shape of the surface being measured. This undeformed shape is used to create FE models as described in Section 2.2.4.

After measuring the undeformed shape, static pressure was applied to the chamber in steps of 0.5 kPa to a maximum of 4 kPa. At each increment, the pressure was held constant and the deformed shape was measured in order to provide data for optimization. This protocol was applied to each contact lens.

2.2.4. FE Model

To construct the FE model, the perimeter of the contact lens, which represents the fixed boundary condition, had to be defined since it was obscured by the cap to simulate a similar situation in eardrums as described earlier. Since the perimeter of the lens was glued to the chamber, the glued boundary of the lens does not move when pressure is applied although the rest of the lens does deform. However, since the perimeter of the surface cannot be measured using the profilometer due to the obscurity, abrupt jumps appear in the measured shapes during the application of pressure as seen in Figure 2.2 which shows profiles through the measured shapes before and after the application of pressure. The pressurized and unpressurized surfaces were extrapolated in the vicinity of the perimeter to a common point of convergence to define the unmeasured perimeter. This was done by fitting cubic B-spline surface patches in the vicinity of the perimeter and extrapolating to a common fixed boundary point. The boundary along with the measured undeformed surface was used to create a mesh suitable for FE analysis. The mesh was generated using the transfinite

interpolation (TFI) method (Knupp and Steinberg, 1993) as described in Section 2.3. The unpressurized mesh produced by the profilometer could not be used directly for FE analysis because it has many ill-formed triangles (e.g., with small internal angles). Moreover, the TFI method uses quadrilateral isoparametric elements which are known to have superior performance compared to triangular elements. The thickness of each element was based on the thickness distribution measured by Marshall *et al* (2007). For the contact lenses used in this study, the thickness is largest at the centre and has a value of 190 μm . It decreases in the radial direction to a minimum value of 95 μm at the periphery. The Poisson's ratio of each element was set to 0.3. The Young's modulus value for each element was identical and was initialized and updated by the optimization routine (Section 2.2.5).

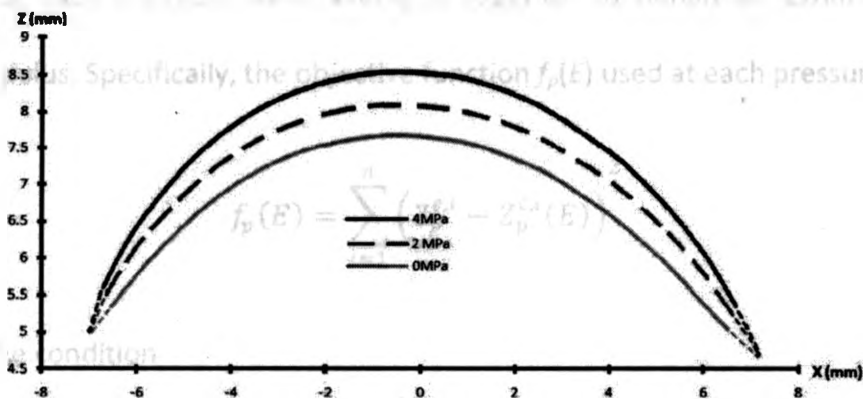


Figure 2.2: Radial profiles through contact lens at different pressures. The small dashed lines show the extrapolation of the profiles which converge at boundary points.

Static pressures identical to those used in the experiment were simulated in the FE modeling software (Abaqus, Simulia Inc., RI, USA), and the Young's modulus of the model was optimized so that calculated pressurized shapes matched experimental measurements as outlined in Section 2.2.5. Furthermore, because the amount of displacement in the pressurization experiments was significant compared to the eardrum's thickness, the FE model was formulated taking into account geometric nonlinearity but assuming linearly elastic material behaviour.

2.2.5. Optimization

The Young's modulus of the lens was estimated by optimizing the value used in the FE model until calculated deformed shapes matched measured shapes. A separate optimization was done at each pressure used in the experiments, and the values estimated at each pressure were averaged together to obtain an estimate of the Young's modulus. Specifically, the objective function $f_p(E)$ used at each pressure p was

$$f_p(E) = \sum_{i=1}^n \left(Z_p^{e,i} - Z_p^{c,i}(E) \right)^2$$

subject to the condition

$$E_l < E < E_u$$

where E is the Young's modulus, $Z_p^{c,i}(E)$ is the Z- coordinate of node i of the FE model calculated at pressure p for a specific value of E and $Z_p^{e,i}$ is the experimentally measured Z-coordinate corresponding to node i of the model at the same pressure. The summation is for all n nodes in the FE model. E is subject to the constraint that it is bounded between a lower value (E_l) and an upper value (E_u). This is a one-dimensional optimization problem that was solved to find the optimal E value using the golden section search algorithm (Press *et al*, 1992). For all contact lenses, E_l was set to vary between 0.1 to 0.8 MPa, and E_u was varied between 2.0 to 4.0 MPa in order to investigate the sensitivity of the optimization algorithm to these parameters.

2.3. Application to Eardrum

In order to demonstrate the applicability of the estimation technique to the eardrum and assess its repeatability, it was applied to six adult rat eardrums. For each rat, the temporal bone was removed 30 min post mortem. The ear canal was resected to within 0.5 mm of the tympanic ring in order to provide a good view of the eardrum for shape measurement. In order to measure the mechanical response of the eardrum without the confounding effects of the ossicular and cochlear loads, the malleus was immobilized by gluing the malleolar head to the middle-ear wall as described elsewhere (Ladak *et al.*, 2004). The eardrum was left intact, i.e., the eardrum was not dissected from its attachments to the ear canal or the manubrium of the malleus. For

pressurization using the pressurization apparatus the temporal bone was drilled to make a small hole leading to the middle ear cavity. A syringe needle was inserted from its tip end into the hole while its other end was connected to the pressurization apparatus. To prevent air leakage two end connections of the syringe were sealed using silicone rubber. The eardrum specimen was coated for shape measurement, the temporal bone was secured in a holder, and the eardrum's pressurized and unpressurized shapes were measured for the same sequence of pressures as used with the contact lenses (see Section 2.2.3) with one modification: The pressurization sequence was applied five times. For each sequence, the pressure was increased from 0 kPa to 4.0 kPa in steps of 0.5 kPa, and then the pressure was reduced back to 0 kPa. Shape measurements were only made during the fifth sequence. The first four sequences were needed to precondition the eardrum.

The eardrum's perimeter was determined using the extrapolation technique described in Section 2.2.4. The unpressurized mesh produced by the profilometer along with the extrapolated perimeter was used to create an FE mesh as outlined here. For reference, a sample mesh is shown in Figure 2.3 with parts of the eardrum labeled. The pars tensa is the main surface of the eardrum, whereas the pars flaccida is a smaller and less stiff portion of the eardrum. The boundary between the two surfaces and the outline of the manubrium (the portion of the malleus bone embedded in the eardrum)

were manually traced by comparison to a digital image of the same specimen. The mesh generation technique we developed for the eardrum is based on the TFI method and involves transforming five rectangular grids in the logical domain to the spatial domain. The five regions in the eardrum's spatial domain are a rectangular domain in the center of the eardrum in addition to four regions, each of which makes up a quarter of the remaining part of the eardrum. This configuration was adapted to obtain quadrilateral FE elements with proper angles. In general, the process of transfinite interpolation for each one of the five regions involves three basic steps. First, the boundary to be meshed is divided into four separate curves, defining for example the left, right, top, and bottom sections of the image. Thus, a logical domain is defined, which is typically a square grid with unit edges. Finally, the transformation of the grid from the logical to the spatial domain is constructed using warping functions that ensure smooth mesh line transitions from left to right and bottom to top. Detailed implementation of this meshing technique is described by O'Hagan and Samani (2008). We used four-noded quadrilateral thin shell elements to model the eardrum. On average, the final mesh for each specimen consisted of 1622 elements and 1728 nodes.

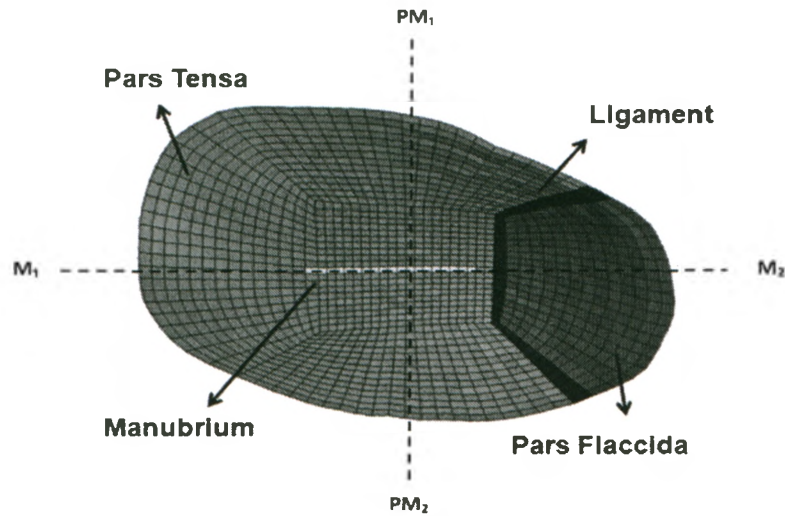


Figure 2.3: Sample FE model of the rat eardrum with its sub-surfaces labeled. The two dashed lines show the cross sections used in creating Figure 2.9.

We focused on estimating the Young's modulus of the pars tensa of the eardrum as it plays a critical role in load transfer from the eardrum to the ossicles. As in previous modeling efforts, the material properties of the model eardrum were assumed to be linearly elastic, homogeneous and isotropic (e.g., Elkhouri *et al.*, 2006). As noted before, these assumptions permit us to specify the material properties of the model eardrum by a Young's modulus value and a Poisson's ratio. The thickness of the pars tensa was taken to have an average uniform thickness of 12 μm based on micro-CT images (Marshall *et al.*, 2007). The Young's modulus value of each element of the pars tensa was taken to be the same and was automatically set and updated by the optimization routine using an initial interval defined by E_l between 1 to 10 MPa and E_u between 30 to 100 MPa. Similar to the pars tensa, the pars flaccida was assumed to have a thickness of 12 μm while its

Young's modulus was constrained to be one-twentieth of that of the pars tensa to make it more compliant than the pars tensa. The boundary between the pars tensa and pars flaccida was modeled as a "ligament". The Young's modulus of this ligament was taken to be 100 MPa based on the properties of other ligaments (Ethier and Simmons, 2007), and its thickness was taken to be 12 μm . The thickness of the manubrium was set to an average value of 100 μm based on a micro-CT scan, and its Young's modulus was set to 15 GPa, which is equivalent to that of cortical bone (Mow and Huiskes, 2005). All tissues were assumed to have a Poisson's ratio of 0.3 (Funnell and Laszlo, 1978). The tympanic ring was assumed to be fully clamped. The superior boundary of the manubrium was assumed to be fully clamped whereas the rest of the manubrial boundary was tightly coupled to the pars tensa. This approximately simulates the experimental condition of immobilizing the malleolar head.

2.4. Results

2.4.1. Validation

Figure 2.4 shows an FE model for one of the contact lenses. This particular model consists of 1520 elements connecting 1561 nodes and incorporates the measured thickness variation measured by Marshall *et al* (2007). The Young's modulus estimated for this lens was 1.34 MPa. Figure 2.5 shows a radial profile (dots) extracted through a shape measurement through the same lens with a pressure of 4 KPa applied; this was

the highest pressure used in the study. The corresponding profile (solid black curve) through the FE model with the deformed shape calculated using the optimal Young's modulus agrees well with the measured shape. Figure 2.6 shows a full-field error map for the same contact lens for a pressure of 4 KPa. The error is defined as $|Z_p^{e,i} - Z_p^{c,i}(E)|$. The largest error occurs close to the periphery but is less than 0.1 mm which is substantially smaller than the largest displacement of the contact lens which was 1.2 mm. The average error computed over the entire surface was 0.004 mm. Similar good agreement between simulated and measured profiles was also found for the lower pressures used in this study. The average Young's modulus measured for the 5 lenses was 1.33 ± 0.02 MPa. These estimates were not sensitive to the choice of E_l or E_u as long as these bounds were chosen to encompass the expected optimal value of the Young's modulus. Figure 2.7 shows the objective function as a function of E , the Young's modulus of the FE model of the contact lens. Note that the function has a single well defined minimum over a large range of Young's moduli.



Figure 2.4: Sample FE model of a contact lens.

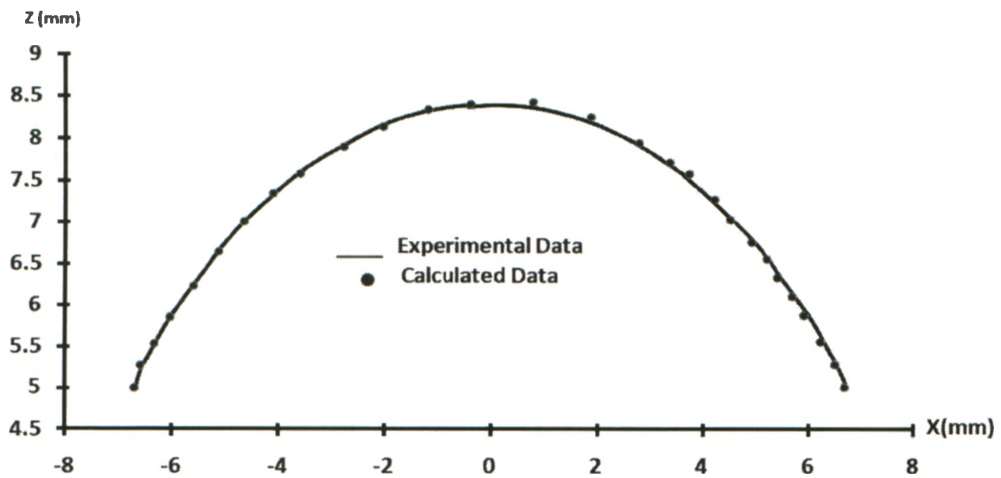


Figure 2.5: Radial profile through pressurized contact lens and through corresponding measurement at 4 KPa.

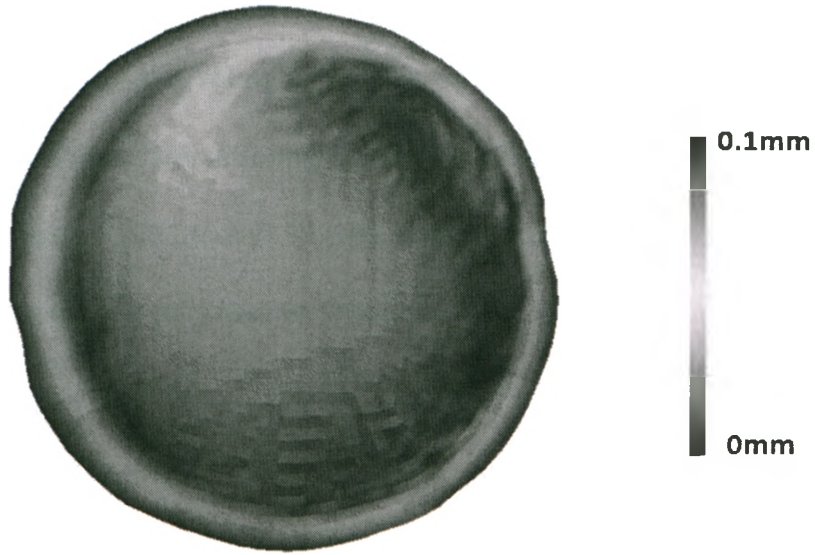


Figure 2.6: Full-field error map of the same contact lens shown in Fig. 2.4 for a pressure of 4 KPa.

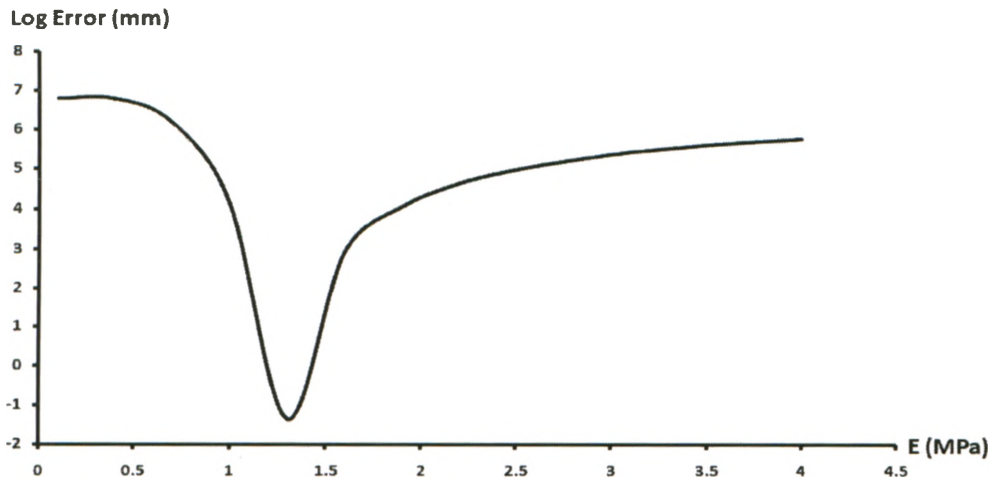


Figure 2.7: Graph of objective function as a function of Young's modulus for the contact lens.

Figure 2.8 shows the effects of assuming a uniform thickness value in the FE model for estimating the Young's modulus as opposed to the varying thickness used above. Based on this graph, a Young's modulus estimated using the average thickness of 142 μm (average of 190 μm and 95 μm) appears to be close to the value estimated by taking into account the thickness variation.

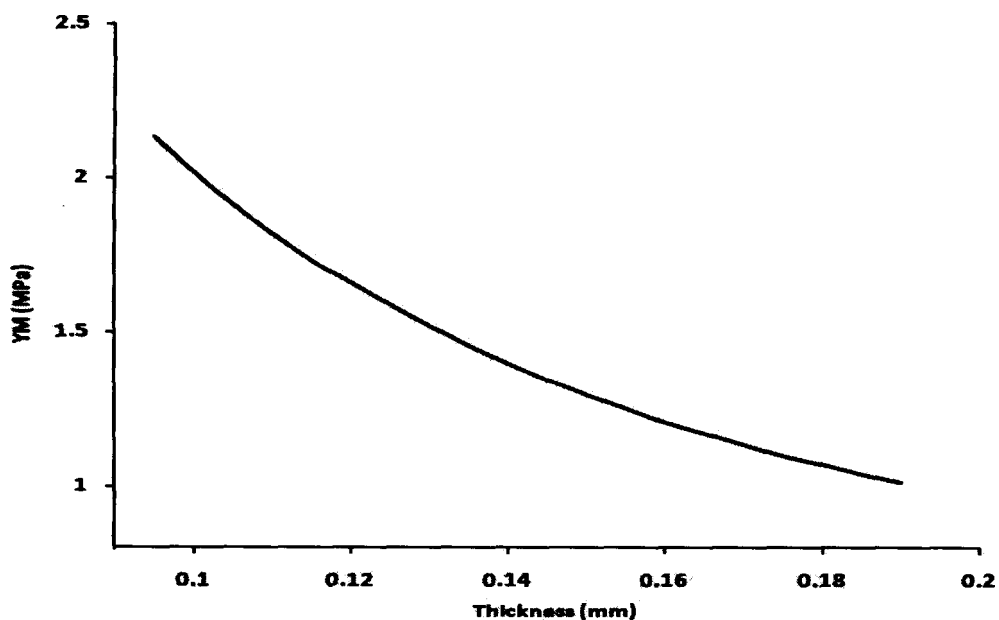


Figure 2.8: Effect of having different uniform thicknesses along the surface of contact lens on calculation of Young's modulus (YM) value.

2.4.2. Application to Eardrum

The Young's modulus value estimated using the eardrum mesh shown in Figure 2.3 was 22.1 MPa. Figure 2.9 shows two shape profiles for a pressure of 4 kPa. The

profile in part (a) is taken midway along the manubrium and perpendicular to it; the location of the profile is shown by the dashed line labeled PM₁-PM₂ in Figure 2.3. The profile in part (b) is taken along the length of the manubrium; the location of the profile is shown by the dashed line labeled M₁-M₂ in Figure 2.3. In both parts (a) and (b) of Figure 2.9, the dotted profile was computed using the optimal Young's modulus value for this specimen. The solid line is the corresponding profile through the shape data measured using the profilometer. The measured and simulated profiles agree well with each other for this pressure except on the area of the pars flaccida [end closest to M₂ in Figure 2.9(a)]. Figure 2.10 shows a full-field error map for the same eardrum for a pressure of 4 KPa. The error is defined as $|Z_p^{e,i} - Z_p^{c,i}(E)|$. The largest error occurs in the pars flaccida and is less than 0.3 mm which is much smaller than the maximum displacement of the eardrum which was 2.1 mm. The maximum error in the pars tensa is less than 0.25 mm. The average error computed over the pars tensa, pars flaccida and the entire eardrum surface is 0.03 mm, 0.1 mm and 0.05 mm respectively. Similar good agreement was also found at all lower pressures and for all specimens. The average Young's modulus measured for the six eardrums was 22.8 ± 1.5 MPa.

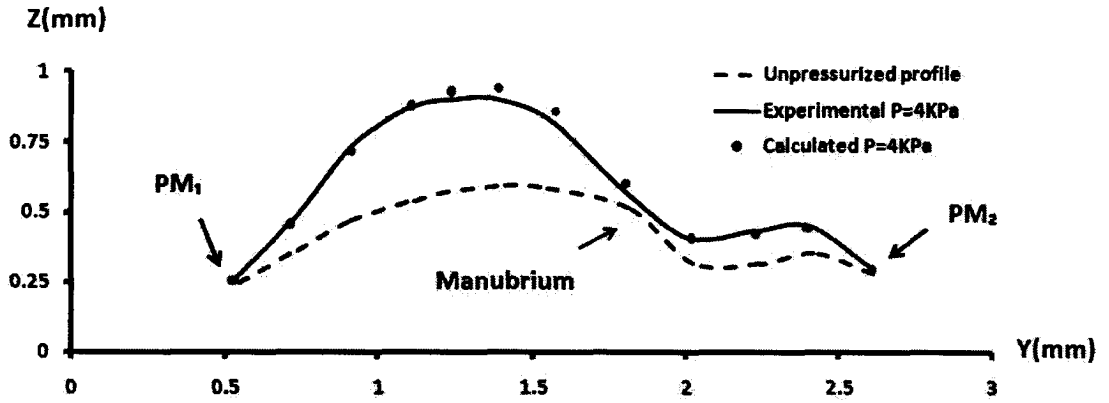


Figure 2.9(a): Shape profiles at midway along manubrium and perpendicular to it; through pressurized eardrum and through corresponding measurement at 4 KPa.

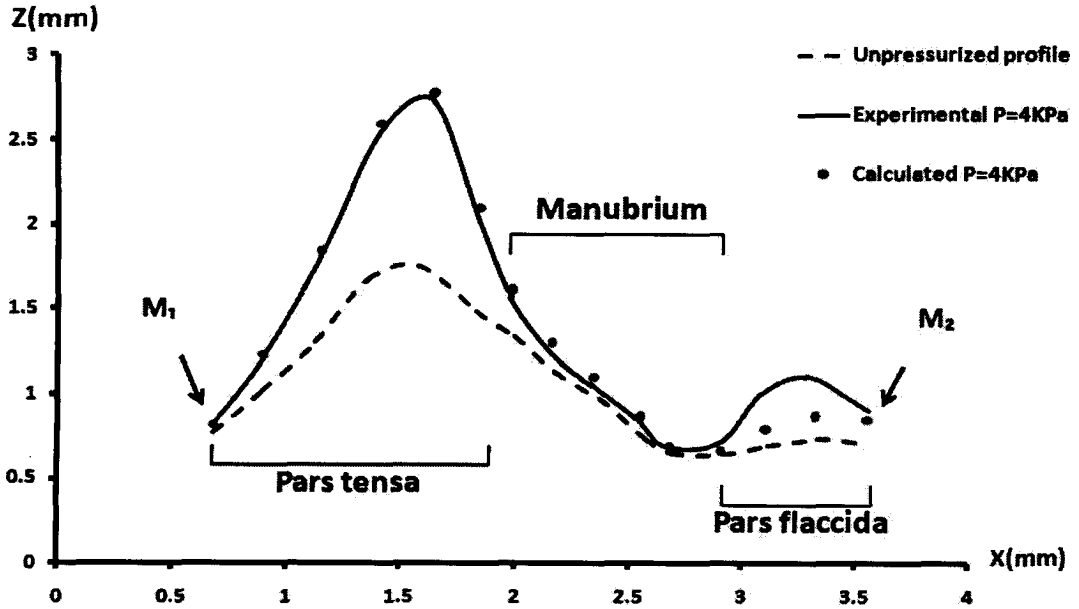


Figure 2.9(b): Shape profiles along manubrium through pressurized eardrum and through corresponding measurement at 4 KPa.

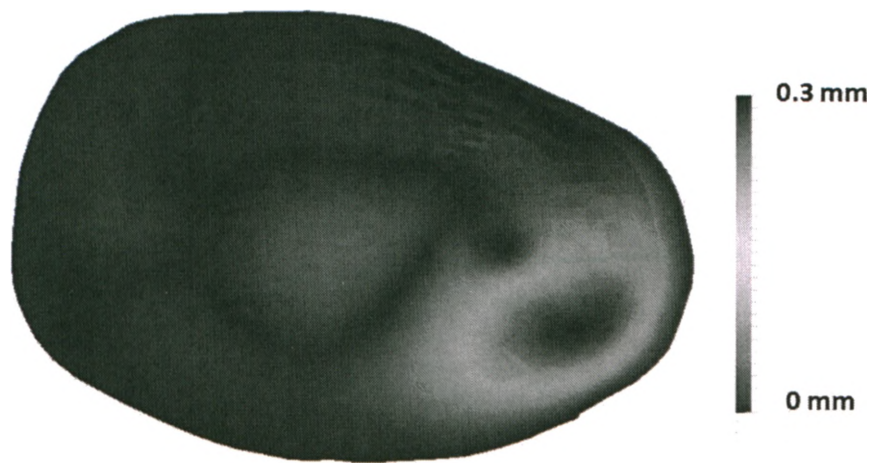


Figure 2.10: Full-field error map of the same eardrum shown in Fig. 2.9 for a pressure of 4 KPa.

These estimates were not sensitive to the choice of E_l or E_u as long as these bounds were chosen to encompass the expected optimal value of the Young's modulus. Figure 2.11 shows the objective function as a function of E , the Young's modulus of the FE model of the eardrum. Note that the function has a single well defined minimum over a large range of Young's moduli.

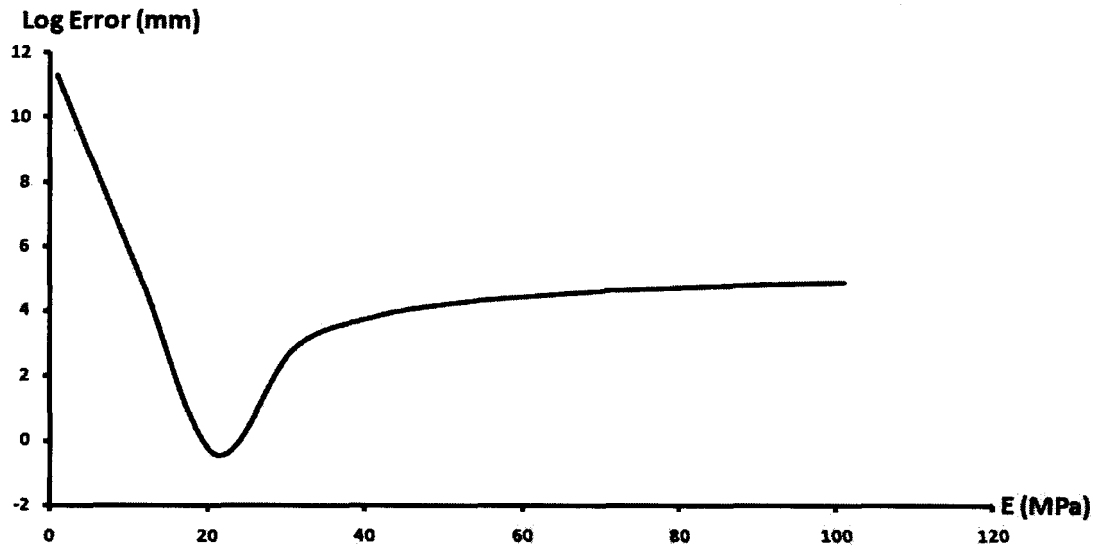


Figure 2.11: Graph of objective function as a function of Young's modulus for the eardrum.

2.5. Discussion

2.5.1. Validation

The estimated average Young's modulus value of 1.33 ± 0.02 MPa for the 5 contact lenses is within the range of 1.2 MPa to 1.4 MPa found in the literature (Summary of Safety and Effectiveness Data 2001; Ross *et al.*, 2005). The low standard deviation is indicative of the repeatability of the technique despite having to extrapolate the periphery of each lens which is obscured by the cap (simulating an equivalent situation for the eardrum). It also reflects the low variability amongst samples. The optimal Young's modulus is insensitive to the initial range as specified by E_l and E_u used in the optimization routine as long as the range encompassed the optimal value.

The measured value is sensitive to the thickness of the contact lens. For the lenses used in this study, the thickness varies from a high value in the centre to lower values at the periphery. Since the thickness distribution of the rat eardrum is not known, we tested the effects of using a uniform thickness value across the surface of one contact lens model to determine the effects of assuming a uniform thickness value. As this uniform value was increased from 95 μm to 190 μm , the estimated Young's modulus decreased. When the thickness of a shell structure increases, its overall structural stiffness also increases. Consequently, the estimated Young's modulus decreases to match the constant structural stiffness of the actual eardrum. Using an average uniform thickness of 142 μm results in an estimated Young's modulus that matches the estimate obtained in a model where the thickness distribution is taken into account.

2.5.2. Application to Eardrum

The estimated average value of the effective Young's modulus of the rat eardrum is 22.8 ± 1.5 MPa. This "effective" value is suitable for use with isotropic models. This effective Young's modulus appears to be good in modeling the behaviour of the pars tensa. However, this value does not produce a good match between simulation and experimental data for the pars flaccida. This is because no attempt was made to separately optimize the Young's modulus of the pars flaccida. Instead, the

Young's modulus of the pars flaccida was arbitrarily constrained to be a fraction of that of the pars tensa to reduce the optimization problem to one dimension. Note that the pars flaccida is a mechanically less important area of the eardrum. The standard deviation in the measurements is relatively low reflecting the repeatability of the technique and low variability amongst the animals used in this study.

This estimate is close to the value of 21.7 ± 1.2 MPa reported by Hesabgar *et al* (2009). As described in Section 2.1, they used an indentation technique to measure eardrum response and estimated the Young's modulus by optimizing an FE model. The pressurization technique used in this work has the advantage that complex contact modeling is not required.

Aernouts *et al* (2009) also used an indentation technique and optimized an FE model. Their results for the rabbit ear are up to 50% higher than ours in the rat. It is not clear if this difference arises due to differences in species. They avoided the need for contact modeling by using a flat-ended cylindrical indenter. Hesabgar *et al* used a spherical-ended indenter for which the contact area grows as the indenter is progressively pushed onto the eardrum. However, a flat-ended indenter can potentially cause damage to soft tissues as was experienced in our lab.

Interestingly, our estimate of the Young's modulus is similar to the static value of 20 MPa measured by Békésy (1960) in portion of the pars tensa cut from a human

cadaver. It would be interesting to apply our technique to the human eardrum to determine if tissue damage induced by cutting as in Békésy's experiment has any effect on the mechanical properties of the eardrum.

The values of quasi-static Young's moduli reported by Gaihede *et al* (2007) are substantially lower than ours and those reported by others. Their experiments involved measuring the volume deformation of the eardrum in response to the application of static pressure and were done *in vivo*, whereas ours and those of others were done in cadaveric tissue. However, the mechanical behaviour of the middle ear does not change significantly several hours or even days after death (Rosowski, 1990) as long as precautions are taken as in our work. In order to estimate the Young's modulus Gaihede *et al* made several assumptions in modeling the eardrum. These include (1) ignoring the curved conical shape of the eardrum and considering the undeformed shape to be a flat circle, (2) modeling the eardrum as one surface by not differentiating between the pars tensa and pars flaccida, (3) ignoring the manubrial attachment to the eardrum and (4) assuming linear behaviour by not accounting for geometric nonlinearity. It is quite likely that these simplifying assumptions lead to differences between their results and those of others.

Estimates of the Young's modulus have been made using dynamic stimuli. Kirikae (1960) performed tensile testing on strips cut from a human eardrum using an

oscillation frequency of 890 Hz and estimated a value of 40 MPa. Using an oscillation frequency of 300 Hz, Decraemer *et al* (1980) estimated a value of 23 MPa. The Young's modulus of soft tissues does vary with frequency (Fung, 1993), so a direct comparison to our work is not possible, although it is worthwhile to note that the low-frequency estimate of Decraemer *et al* (1980) in the human eardrum is close to that of ours in the rat.

Fay *et al* (2005) estimated the Young's modulus of the eardrum taking into account the layered fibrous ultrastructure of the eardrum using three different approaches: constitutive modeling, re-interpretation of previous measurements made by Békésy, Kirikae and Decraemer *et al*, and finally through their own dynamic measurements. Their values (0.1 to 0.3 GPa in humans and 0.1 to 0.4 GPa in cats) are substantially higher than the estimates of others, including us. Their approach requires quantitative knowledge of the distribution and density of fibers in the eardrum which is not well known; however, effort is underway to gather this information (Jackson *et al* 2009).

A highly relevant work is that of Huang *et al* (2008) in which the authors estimate the in-plane and through-thickness Young's "relaxation" modulus of the human eardrum. This is a measure of the Young's modulus at various instants of time during a relaxation experiment. In the steady-state, they estimated a through-thickness value of

6.0 MPa for both the posterior and anterior pars tensa and in-plane values of 17.4 MPa and 19.0 MPa for the posterior and anterior pars tensa, respectively. The Young's modulus of relaxation varies with time. For instance, in the posterior pars tensa, this quantity varies from 22.8 MPa at 5 sec after the application of loading to 17.4 MPa in steady state. Our measurements were done in the posterior pars tensa and are in agreement with the earlier part of their range since in our experiment, shape measurements were made within 5 sec of applying pressure.

The sensitivity analysis conducted by Hesabgar *et al* (2009) indicates that this type of optimization approach to estimating the Young's modulus is sensitive to the thickness of the pars tensa. Our analysis for a contact lens (see Figure 2.8) suggests that using an average thickness value that is uniform across the surface being modeled can yield results similar to models incorporating variation in thickness. The applicability of this to the eardrum needs to be tested; however, measurement of eardrum thickness distribution is difficult, but has recently been done in humans (Kuypers *et al*, 2003), gerbils (Kuypers *et al*, 2005) and rabbits (Kuypers *et al*, 2000).

2.6. Conclusion

A technique to estimate the Young's modulus of curved shell-like structures was presented in which the resting and pressurized shapes were measured using a Fourier transform profilometer. FE meshes with subject-specific geometries were generated

from the resting shape data and the pressurization experiment was simulated. The Young's modulus of the FE model was numerically optimized until simulated pressurized shapes matched measured ones. The technique was evaluated on contact lenses with known Young's moduli values and was shown to provide accurate and highly reproducible estimates. The estimated Young's modulus of the healthy adult rat eardrum was found to be $22.8 \text{ MPa} \pm 1.5 \text{ MPa}$, which is comparable to some of the values found in the literature for the human eardrum. Moreover, the proposed technique is highly reproducible.

2.7. References

- Aernouts, J.E.F., Soons, J.A.M., Dirckx, J.J.J., 2009. Quantification of tympanic membrane elasticity parameters from in situ measurements. MEMRO 2009 5th International Symposium, Stanford University, California, U.S.A.
- Beer, H.-J., Bornitz, M., Hardtke, H.-J., Schmidt, R., Hofmann, G., Vogel, U., Zahnert, T., Hüttenbrink, K.-B., 1999. Modelling of components of the human middle ear and simulation of their dynamic behaviour. *Audiol. Neuro-otol.*, 4 (3-4) 156-162.
- Békésy, G.v., 1960. *Experiments in Hearing*, McGraw-Hill, Toronto, ON.
- Decraemer, W.F., Maes, M.A., Vanhuysse, V.J., 1980. An elastic stress-strain relation for soft biological tissues based on a structural model., *J. Biomech.*, 13 (6) 463-468.
- Dirckx, J. J. J., Decraemer W. F., 1997. Coating techniques in optical interferometric metrology. *Appl. Opt.* 36 2776-2782

- Eiber, A., 1999. Mechanical modeling and dynamical behaviour of the human middle ear. *Audiol. Neuro-otol.*, 4 (3-4) 170-177.
- Elkhouri, N., Liu, H., Funnell, W.R.J., 2006. Low-frequency finite-element modelling of the gerbil middle ear. *J. Assoc. Res. Otolaryngol.*, 7 (4) 399-411.
- Ethier, C.R. and Simmons, C.A., 2007. *Introductory Biomechanics from Cells to Organisms*, Cambridge University Press, Cambridge, UK.
- Fay, J., Puria, S., Decraemer, W.F., Steele, C., 2005, Three approaches for estimating the elastic modulus of the tympanic membrane. *J. Biomech.*, 38 (9) 1807-1815.
- Ferris, P.; Prendergast, P.J., 1999. Middle-ear dynamics before and after ossicular replacement. *J. Biomech.*, 33 (5) 581-590.
- Fried, M.P., Uribe, J.I., Sadoughi, B., 2007. The role of virtual reality in surgical training in otorhinolaryngology, *Curr. Opin. Otolaryngol. Head Neck Surg.*, 15(3) 163-169.
- Fung, Y.C., 1993. *Biomechanics: Mechanical Properties of Living Tissues*, 2nd ed., Springer-Verlag, New York City, NY.
- Funnell, W.R.J., Decraemer, S.M., Khanna, J., 1987. On the damped frequency response of a finite-element model of the cat eardrum. *J. Acoust. Soc. Am.*, 81 (6) 1851-1859.
- Funnell, W.R.J., Laszlo, C.A., 1978. Modeling of the cat eardrum as a thin shell using the finite-element method. *J. Acoust. Soc. Am.*, 63 (5) 1461-1467.
- Funnell, W.R.J., Laszlo C.A., 1982. A critical review of experimental observations on eardrum structure and function. *ORL*, 44(4) 181-205

- Gaihede, M., Liao, D., Gregersen, H., 2007. *In vivo* areal modulus of elasticity estimation of the human tympanic membrane system: modelling of middle ear mechanical function in normal young and aged ears. *Phys. Med. Biol.*, 52 (3) 803-814.
- Huang, G., Daphalapurkar, N.P., Gan, R.Z., Lu, H., 2008, A Method for measuring linearly viscoelastic properties of human tympanic membrane using nanoindentation. *J. Biomech. Eng.*, 130 (1) 014501.
- Jackson, R.P., Ricci, T., Chlebicki, C., Krasieva, T.B., Zalpuri, R., Triffo, W.J., Puria, S., 2009, Multiphoton and electron microscopy of collagen in ex vivo, human tympanic membranes, MEMRO 2009 5th International Symposium, Stanford University, California, U.S.A.
- Kirikae, I., 1960. *The Structure and Function of the Middle Ear*. University of Tokyo Press, Tokyo.
- Knupp, P., Steinberg, S., 1993. *Fundamentals of Grid Generation*, CRC Press, Boca Raton, FL.
- Koike, T., Wada, H., Kobayashi, T., 2002. Modeling of the human middle ear using the finite-element method. *J. Acoust. Soc. Am.*, 111 (3) 1306-1317.
- Kuypers, L.c., Decraemer, W.F., Dirckx, J.J.J., 2003. Thickness of the human eardrum in fresh and preserved specimens. *Middle ear mechanics in research and otology 3rd symposium*, Matsuyama, Ehime, Japan.
- Kuypers L.C., Dirckx J.J.J. , Decraemer W.F.,2000. Eardrum thickness measured on confocal microscope virtual sections. *Assoc. Res. Otolaryngol. Abs.:* 4140
- Kuypers, L.C., Dirckx, J.J.J., Decraemer, W.F., 2005. Thickness of the gerbil tympanic membrane measured with confocal microscopy. *Hearing Research*. 209(1-2) 42-52

- Ladak, H.M., Dirckx, J.J.J., Decraemer, W.F., Funnell, W.R.J., 2004. Response of the cat eardrum to static pressures: Mobile versus immobile malleus. *J. Acoust. Soc. Am.*, 116 (5) 3008-3021.
- Ladak, H.M., Funnell, W.R.J., Decraemer, W.F., Dirckx, J.J.J., 2006. A geometrically nonlinear finite-element model of the cat eardrum. *J. Acoust. Soc. Am.*, 119 (5) 2859-2868.
- Leigh, S., Govind, R., Husein, M., Doyle, P., Agrawal, S., Ladak, H., 2009, Development and face validity testing of a three dimensional myringotomy simulator with haptic feedback. *J. Otolaryngol.*, in press.
- Marshall, H.R., Ladak, H.M., Samani, A., 2007. A finite element model based approach to determine the Young's modulus of the intact tympanic membrane, CompMed, Montreal, Quebec, Canada.
- Mow, V.C., Huiskes, R., 2005. *Basic Orthopaedic Biomechanics and Mechano-Biology*, Third Edition, Lippincott Williams and Wilkins, PA.
- O'Hagan, J. J., Samani, A., 2008. Measurement of the hyperelastic properties of tissue slices with tumour inclusion. *Phys. Med. Biol.*, 53 (24) 7087-7106.
- Pokras, R., Kozak, L.J., McCarthy E., 1997. Ambulatory and inpatient procedures in the United States, 1994. *Vital Health Stat.*, 13(132) 11-17.
- Press, W.H., Teukolsky, S.A., Vetterling, W.T., Flannery, B.P., 1992. *Numerical Recipes in Fortran 77, The Art of Scientific Computing*, Cambridge University Press, Cambridge.
- Rosowski, J.J., 1990. Cadaver middle ears as models for living ears: Comparisons of middle ear input immittance. *Ann. Otol. Rhinol. Laryngol.*, 99 (5 Pt 1) 403-412.

Ross, G, Nasso, M, Franklin, V, Lydon, F and Tighe, B Silicone 2005 Hydrogels: Trends in Products and Properties BCLA 29th Clinical Conference & Exhibition

Summary of Safety and Effectiveness Data (lotrafilcon A hydrophilic contact lens)
October 12, 2001 P000030 : FDA

Tuck-Lee, J.P., Pinsky, P.M., Steele, C.R., Puria, S., 2008. Finite element modeling of acousto-mechanical coupling in the cat middle ear. *J. Acoust. Soc. Am.*, 124 (1) 348-362.

Chapter 3

Summary, Conclusion and Future Work

3.1. Summary

This research tackled the problem of measuring the *ex vivo* quasi-static YM of the eardrum where the rat was used as an animal model. For this purpose a novel measurement system was developed which involved applying known air pressure to rat's *ex vivo* eardrum while measuring its response. This response was characterized by the shape change of the eardrum measured based on the pre- and post pressurization shapes of the eardrum. These shapes were acquired using a 3D profilometer. The advantage of the proposed technique is that it does not require tissue dissection; hence the measurement procedure does not compromise the tissue structural integrity. Furthermore, unlike some other measurement techniques, the proposed technique incorporates many details in the FE model, e.g. the manubrium, pars flaccida and the ligament separating the pars tensa from the pars flaccida. This technique was validated using a phantom study before it was applied to a small number of rat eardrum specimens. The technique proved to be both repeatable and reasonably accurate. Developments of this research can be summarized as follows.

3.1.1. Contact Lens Phantom Study

We conducted a phantom study to validate the proposed technique. For this purpose five CIBA Night and Day soft contact lenses were used. Each contact lens was pressurized up to 4 KPa using a pressurization apparatus. The 3D geometry of the contact lens at each pressure applied starting from 0 kPa was acquired by a 3D profilometer (a non-contacting optical device for shape measurements with accuracy up to 10 μm). Subsequently, an FE model was created by incorporating the measured geometry and thickness distribution information. Finally, the YM value of the FE model was varied using the optimization method until the calculated deformed shape of the contact lens matched its measured counterpart. The average YM value obtained for this type of contact lens was 1.33 ± 0.02 MPa which is in a very good agreement with the values reported for this particular type of contact lens (1.2 MPa to 1.4 MPa).

3.1.2. Rat Eardrum Study

The final phase of the project involved measuring the YM of a small statistical sample of six fresh rat eardrum specimens. In this study, after immobilizing the malleus of each ear, quasi static pressure of up to 4 KPa was applied and the deformed shape was measured using the 3D profilometer. Using the non-deformed shape of each specimen and a thickness value of 12 μm , an FE model was constructed and incorporated into the optimization based YM reconstruction algorithm. This study led to

an average YM value of 22.8 ± 1.5 MPa. This value is within the range of values previously reported in the literature.

3.2. Discussion and Future Work

The proposed technique led to YM values that fall within previously reported range. Comparison between the proposed technique with major techniques presented in the literature and the corresponding YM results was discussed in detail in Chapter 2. It was concluded that differences can be attributed to issues related to the use of experimental protocols and the eardrum models. In the proposed technique attempts have been made to address many experimental and modeling issues to obtain YM values that can be reliably used in FE modeling of the middle ear. To further improve the measurement technique, the following issues can be addressed in future studies.

3.2.1. Thickness Distribution

A sensitivity analysis conducted for a related technique for estimation of the YM using indentation testing and inverse FE modeling indicates that the measured eardrum's YM is highly sensitive to the thickness of the pars tensa (Hesabgar *et al*, 2009). In the present study, a uniform thickness with a value of $12 \mu\text{m}$ was used. While this is an acceptable average value according to the literature, incorporating thickness variation across the surface of the pars tensa may lead to higher accuracy. In the

present study for the contact lens, the thickness of the model was based on the thickness distribution measured by Marshall *et al* (2007). For the rat eardrum we assumed a uniform thickness of 12 μm along the surface based on micro-CT images (Marshall *et al*, 2007). One option to obtain accurate thickness distribution is to utilize confocal microscopy (Kuypers *et al*, 2003) for constructing a more accurate FE model for the eardrum.

3.2.2. Inhomogeneity

Another factor that was not taken into account in the FE model is eardrum inhomogeneity. In this research, it was assumed that the rat eardrum is homogeneous throughout its volume whereas in reality there is some deviation from homogeneity. This inhomogeneity can be assessed and taken into account if necessary by dividing the eardrum's structure into a number of regions with distinct unknown YM. This problem leads to more unknown parameters likely significant ill-conditioning in addition to uniqueness issues that need to be tackled properly.

3.2.3. Anisotropy

In the FE model used in the present research, it was assumed that the eardrum tissue is isotropic. However, the eardrum tissue is a four-layer composite (Lim, 1995), which implies anisotropic behavior. While this is true, other researchers have concluded that including anisotropy does not change the basic displacement pattern as compared

to an isotropic model (Funnell and Laszlo, 1978). Furthermore, there is no accurate data on the level of anisotropy in the literature and the extent to which this simplification may alter the YM value. To assess tissue anisotropy, one may incorporate anisotropic constitutive model in the FE model of the present estimation technique. This anisotropic constitutive model should be selected in accordance with the known layered structure of the eardrum tissue. Once again adding this level of complexity to the FE model will lead to a larger number of unknowns and consequently ill-conditioning and uniqueness issues that need to be addressed properly.

3.2.4. Tissue Intrinsic Nonlinearity

In this research, while geometric nonlinearity of the eardrum was considered tissue intrinsic nonlinearity was not considered as the behavior was idealized by linear elastic model. There are some biomedical applications where the eardrum undergoes large deformations and it needs to be modeled as such. One example is for simulating surgeries such as myringotomy for developing VR environments.

3.2.5. Further Eardrum's FE Model Refinement

As described earlier, the eardrum consists of pars flaccida, pars tensa and is attached to manubrium. The mechanical properties of each of these components are known to be dissimilar. The pars flaccida is known to be less stiff compared to the pars tensa while the ligament between them is much stiffer than both the pars tensa and pars flaccida. Given lack of information on the mechanical properties of these tissues,

reasonable values were assumed in the FE model. To improve the measurement accuracy, these variables can be considered. For this purpose, future works in this area would involve setting up an experiment in a way that each time the eardrum is stimulated, only one structure component is affected such that the mechanical properties of each one of them can be assessed separately. Another possibility is to consider a number of unknowns while applying a number of mechanical stimulations to obtain equations necessary to solve for the unknown parameters.

3.3. References

- Funnell, W.R.J., Laszlo, C.A., 1978. Modeling of the cat eardrum as a thin shell using the finite-element method. *J. Acoust. Soc. Am.*, 63 (5) 1461-1467.
- Hesabgar, S.M., Agrawal, S.K., Samani, A., Ladak, H.M., 2009. Measuring the quasi-static Young's modulus of the eardrum using an indentation technique. MEMRO 2009 5th International Symposium, Stanford University, California, U.S.A.
- Kuypers, L.C., Decraemer, W.F., Dirckx, J.J.J., 2003. Thickness of the human eardrum in fresh and preserved specimens. *Middle ear mechanics in research and otology 3rd symposium*, Matsuyama, Ehime, Japan.
- Lim, D.J., 1995. Structure and function of the tympanic membrane: a review. *Acta Oto-Rhino-Laryngologica Belgica.*, (49) 2 101-15

Marshall, H.R., Ladak, H.M., Samani, A., 2007. A finite element model based approach to determine the Young's modulus of the intact tympanic membrane, CompMed, Montreal, Quebec, Canada.